

# 3-flavor and 4-flavor implications of the latest T2K and NO $\nu$ A electron (anti-)neutrino appearance results

Antonio Palazzo<sup>a,1</sup>

<sup>a</sup>Max-Planck-Institut für Physik (Werner Heisenberg Institut), Föhringer Ring 6, 80805 München, Germany

---

## Abstract

The two long-baseline experiments T2K and NO $\nu$ A have recently presented new findings. T2K has shown the first  $\bar{\nu}_e$  appearance data while NO $\nu$ A has released the first  $\nu_e$  appearance results. These data are of particular importance because they allow us to probe for the first time in a direct (or manifest) way the leptonic CP-violation. In fact, it is the first time that a hint of CP-violation arises from the comparison of the observations of neutrinos and antineutrinos. We consider the implications of such new results both for the standard 3-flavor framework and for the non-standard 3+1 scheme involving one sterile neutrino species. The 3-flavor analysis shows a consolidation of the previous trends, namely a slight preference for  $\sin \delta < 0$ , disfavoring CP conservation ( $\delta = 0, \pi$ ) with a statistical significance close to 90% C.L., and a mild preference (at more than 68% C.L.) for the normal hierarchy. In a 3+1 framework, the data constrain two CP-phases ( $\delta_{13} \equiv \delta$  and  $\delta_{14}$ ), which exhibit a slight preference for the common value  $\delta_{13} \simeq \delta_{14} \simeq -\pi/2$ . Interestingly, in the enlarged four neutrino scheme the preference for the normal hierarchy found within the 3-flavor framework completely disappears. This indicates that light sterile neutrinos may constitute a potential source of fragility in the capability of the two LBL experiments of discriminating the neutrino mass hierarchy.

---

## 1. Introduction

Neutrino physics is entering a new era. After the discovery of a relatively large value of  $\theta_{13}$ , the determination of leptonic CP violation (CPV) and the identification of the neutrino mass hierarchy (NMH) have become realistic targets. In this respect, the long-baseline (LBL) experiments represent the first setups able to probe these properties. One of them (T2K), already operative since 2011, has provided the first observation of the conversion of muon neutrinos into electron neutrinos [1]. This result, in combination with the precise determination of the third mixing angle  $\theta_{13}$  achieved with the dedicated reactor experiments [2, 3, 4], has provided the first *indirect* information on CPV. In fact,

---

*Email address:* palazzo@mpp.mpg.de (Antonio Palazzo)

<sup>1</sup>Currently at Dipartimento Interateneo di Fisica “Michelangelo Merlin”, Università di Bari, Via G. Amendola 173, I-70126 Bari, Italy.

all the recent global [5, 6, 7] and partial [8, 9] (including only reactor and T2K data) fits indicate a slight preference for CPV, with a best fit value of the fundamental CP-phase  $\delta$  close to the value  $-\pi/2$ .

A few weeks ago the T2K experiment has presented the first appearance results in the antineutrino channel [10, 11]. In the same days the experiment NOvA has released the first appearance data in the neutrino channel [12]. Although both measurements have a limited statistical power it is nonetheless interesting to consider their impact on the preexisting scenario. With this purpose, we here present both a 3-flavor and a 4-flavor analysis of the results of the two long-baseline experiments, updating our previous work [8].

We underline that the latest T2K and NOvA data considered in the present work are of particular importance. Arguably, they represent the most important piece of information in the current neutrino landscape. In fact, these data allow us to probe for the first time in a direct (or manifest) way the leptonic CPV. It is the first time that a hint of CPV arises from the comparison of the observations of neutrinos and antineutrinos. In contrast, in all the previous analyses the indication on the CP-phase  $\delta$  was indirect, since it arose from the combination of long-baseline (T2K) data and reactor data (Daya-Bay, RENO and Double-Chooz). Our analysis shows that the role of reactor data, albeit still significant, is now less pronounced in determining the estimate of the CP-phase  $\delta$ . This trend is likely to be reinforced in the future since the current LBL appearance data represent only a small fraction ( $\sim 10\%$ ) of their total planned exposure.

We recall that the LBL experiments are sensitive to CPV because they can probe the interference of two distinct oscillating frequencies. In the 3-flavor case, the two frequencies in question are related to the atmospheric squared-mass splitting and to the solar one. In the 4-flavor case, the interference occurs between the fast (averaged) oscillations induced by the new  $O(\text{eV}^2)$  splitting and the atmospheric one. As first shown in [8], the new interference term has an amplitude comparable to that of the standard 3-flavor one. Therefore, it is possible to extract from LBL experiments<sup>2</sup> some information on the enlarged CPV sector involved in the 3+1 scheme.<sup>3</sup> In particular, it was shown that the data preferred the common value  $\delta_{13} \simeq \delta_{14} \sim -\pi/2$  (where  $\delta_{13} \equiv \delta$ ). Such a behavior was essentially driven by the slight mismatch existing between the two determinations of  $\theta_{13}$  achieved respectively with reactor and T2K data.

We also recall that the LBL experiments are sensitive to the NMH because of the MSW effect [25, 26], which induce (tiny) modifications of the mass-mixing parameters in matter that depend on the sign of the atmospheric splitting. In a sense, also this phenomenon may be regarded as a kind of interference, occurring between the MSW potential (whose sign is known) and the atmospheric squared-mass splitting (whose sign is unknown and to be determined). The same phenomenon is at the basis of the planned measurements of the NMH with atmospheric neutri-

---

<sup>2</sup>For other recent studies addressing the issue of sterile neutrinos at LBL experiments see [13, 14, 15]. Previous related works can be found in [16, 17, 18, 19, 20, 21, 22, 23, 24].

<sup>3</sup>In principle, also the atmospheric neutrinos may provide some information on the enlarged CPV sector, since they traverse very long distances in their path through the Earth.

nos [27, 28, 29, 30], where there is the advantage that the CPV interference effects are less important and there is no degeneracy among the determination of CPV and NMH, which instead notoriously plagues the LBL measurements. It is worth mentioning that the interference of the MSW matter potential with the atmospheric frequency is also present in the propagation of solar neutrinos (see for example [31]), but unfortunately its amplitude is too small to extract any useful information from it (at least with the present data).

Our 3-flavor fit evidences a consolidation of the previous hints, namely a slight preference for  $\sin \delta < 0$  and a mild preference (at more than 68% C.L.) for the normal hierarchy. In a 3+1 framework, the data are able to constrain two (of the three) CP-phases ( $\delta_{13} \equiv \delta$  and  $\delta_{14}$ ), which exhibit a slight preference for the common value  $\delta_{13} \simeq \delta_{14} \simeq -\pi/2$ . Interestingly, in the enlarged four neutrino scheme the preference for the normal hierarchy found within the 3-flavor framework completely disappears. This occurs because the mismatch between the two estimates of  $\theta_{13}$  provided by reactor and LBL experiments (more pronounced in the IH case) can be “cured” with an appropriated choice of the new CP-phase  $\delta_{14}$ . This circumstance indicates that light sterile neutrinos may constitute a potential source of fragility in the capability of the two LBL experiments of discriminating the neutrino mass hierarchy.

The rest of the paper is organized as follows. In Sec. II we introduce the theoretical framework needed to discuss the analytical behavior of the LBL  $\nu_\mu \rightarrow \nu_e$  and  $\bar{\nu}_\mu \rightarrow \bar{\nu}_e$  transition probabilities in the 3-flavor and 4-flavor frameworks. In Sec. III we present the results of the numerical analysis. Finally, in Sec. IV we draw our conclusions.

## 2. Theoretical framework

In the presence of a fourth sterile neutrino  $\nu_s$ , the flavor and the mass eigenstates are connected through a  $4 \times 4$  mixing matrix. A convenient parameterization of the mixing matrix is

$$U = \tilde{R}_{34} R_{24} \tilde{R}_{14} R_{23} \tilde{R}_{13} R_{12}, \quad (1)$$

where  $R_{ij}$  ( $\tilde{R}_{ij}$ ) represents a real (complex)  $4 \times 4$  rotation in the  $(i, j)$  plane containing the  $2 \times 2$  submatrix

$$R_{ij}^{2 \times 2} = \begin{pmatrix} c_{ij} & s_{ij} \\ -s_{ij} & c_{ij} \end{pmatrix} \quad \tilde{R}_{ij}^{2 \times 2} = \begin{pmatrix} c_{ij} & \tilde{s}_{ij} \\ -\tilde{s}_{ij}^* & c_{ij} \end{pmatrix}, \quad (2)$$

in the  $(i, j)$  sub-block, with

$$c_{ij} \equiv \cos \theta_{ij} \quad s_{ij} \equiv \sin \theta_{ij} \quad \tilde{s}_{ij} \equiv s_{ij} e^{-i\delta_{ij}}. \quad (3)$$

The parameterization in Eq. (1) enjoys the following properties: i) For vanishing mixing with the fourth state ( $\theta_{14} = \theta_{24} = \theta_{34} = 0$ ) it returns the 3-flavor matrix in its usual parameterization. ii) The leftmost positioning of the matrix  $\tilde{R}_{34}$  makes the vacuum  $\nu_\mu \rightarrow \nu_e$  conversion probability independent of  $\theta_{34}$  (and the related CP-phase  $\delta_{34}$ ). iii) For small values of  $\theta_{13}$  and of the mixing angles involving the fourth mass eigenstate, one has  $|U_{e3}|^2 \simeq s_{13}^2$ ,  $|U_{e4}|^2 = s_{14}^2$  (exact),  $|U_{\mu 4}|^2 \simeq s_{24}^2$  and  $|U_{\tau 4}|^2 \simeq s_{34}^2$ , with a clear physical interpretation of the new mixing angles.

Let us now come to the transition probability relevant for T2K and NO $\nu$ A. From the discussion made in [8], it emerges that the conversion probability can be approximated as the sum of three terms

$$P_{\mu e}^{4\nu} \simeq P^{\text{ATM}} + P_{\text{I}}^{\text{INT}} + P_{\text{II}}^{\text{INT}}. \quad (4)$$

The first term represents the positive definite atmospheric transition probability, the second term is related to the standard solar-atmospheric interference, while the third term is driven by the atmospheric-sterile interference. The probability depends on the three mixing angles  $s_{13}, s_{14}, s_{24} \simeq 0.15$ , which can be all assumed to be of the same order  $\epsilon$  and on the ratio of the solar and atmospheric squared-mass splittings  $\alpha \equiv \Delta m_{12}^2 / \Delta m_{13}^2 \simeq \pm 0.03$ , which is of order  $\epsilon^2$ . Keeping terms up to the third order, in vacuum, one finds

$$P^{\text{ATM}} \simeq 4s_{23}^2 s_{13}^2 \sin^2 \Delta, \quad (5)$$

$$P_{\text{I}}^{\text{INT}} \simeq 8s_{13}s_{12}c_{12}s_{23}c_{23}(\alpha\Delta) \sin \Delta \cos(\Delta + \delta_{13}), \quad (6)$$

$$P_{\text{II}}^{\text{INT}} \simeq 4s_{14}s_{24}s_{13}s_{23} \sin \Delta \sin(\Delta + \delta_{13} - \delta_{14}), \quad (7)$$

where  $\Delta \equiv \Delta m_{13}^2 L / 4E$  is the atmospheric oscillating frequency, which depends on the baseline  $L$  and the neutrino energy  $E$ .

The matter effects slightly modify the transition probability, introducing a dependency on the ratio

$$\nu = \frac{V}{k} \equiv \frac{2VE}{\Delta m_{13}^2}, \quad (8)$$

where

$$V = \sqrt{2}G_F N_e \quad (9)$$

is the (constant) matter potential along the neutrino trajectory. Both in T2K and in NO $\nu$ A the value of  $\nu$  is relatively small, being  $\nu \sim 0.05$  in T2K, and  $\nu \sim 0.17$  in NO $\nu$ A, where we have taken as a benchmark the peak energy of the two neutrino beams ( $E = 0.6$  GeV in T2K,  $E = 2$  GeV in NO $\nu$ A). Therefore, it is natural to treat  $\nu$  as a small parameter

of order  $\epsilon$ . The probability in matter can be simply obtained (see the appendix in [8] and the works [32, 33, 34]) by making in the vacuum expression the following substitutions

$$s_{13} \rightarrow s_{13}^m, \quad \Delta \rightarrow \Delta^m, \quad (10)$$

where  $s_{13}^m$  and  $\Delta^m$  represent the mixing angle  $s_{13}$  and the atmospheric oscillation frequency in matter, which for small values of  $\nu$ , take the form

$$s_{13}^m \simeq (1 + \nu)s_{13}, \quad (11)$$

$$\Delta^m \simeq (1 - \nu)\Delta. \quad (12)$$

It can be shown that at the peak energy, where  $|\Delta| \simeq \pi/2$ , the substitutions in Eqs. (10) - (12) produce third order corrections only in the atmospheric term, which reads

$$P_m^{\text{ATM}} \simeq (1 + 2\nu)P^{\text{ATM}}, \quad (13)$$

while the same substitutions in the two interference terms produce only corrections of the fourth order.

The swap of the NMH is parametrized by the replacements

$$\Delta \rightarrow -\Delta, \quad \alpha \rightarrow -\alpha, \quad \nu \rightarrow -\nu. \quad (14)$$

One can observe that, while in general, the two interference terms are not invariant under a swap of the NMH, around the oscillation maximum  $|\Delta| = \pi/2$ , such an invariance is approximately valid. Therefore, in practice the effect of the NMH swap is captured by the modification of the leading term in Eq. (13). Due to the change of sign of  $\nu$ , the transition probability (which acquires the dominant contribution from the atmospheric term) increases (decreases) with respect to the vacuum case in the NH (IH) case. NO $\nu$ A is expected to be more sensitive than T2K to the NMH because of the larger value of the ratio  $\nu$ .

Finally, we recall that the transition probability for antineutrinos is obtained from that of neutrinos by changing the sign of the MSW potential  $V$  and of all the CP-phases. This, for a given choice of the NMH, corresponds to the substitutions

$$\delta_{13} \rightarrow -\delta_{13}, \quad \delta_{14} \rightarrow -\delta_{14}, \quad \nu \rightarrow -\nu. \quad (15)$$

In the NH case  $\nu > 0$  for neutrinos and  $\nu < 0$  for antineutrinos. According to Eq. (13), in the NH case the leading contribution to the transition probability will increase (decrease) for neutrinos (antineutrinos). In the IH case the opposite conclusion holds. When passing from neutrinos to antineutrinos, the first interference term (around the oscillation maximum) changes sign, since it is essentially proportional to  $-\sin \delta_{13}$ . In contrast, the second interference term remains approximately invariant, since it depends on  $\cos(\delta_{13} - \delta_{14})$ .

Remarkably, for typical values of the mixing angles preferred by the current global 3+1 fits, the amplitude of the (atmospheric-sterile) interference term is almost identical to that of the standard (solar-atmospheric) interference term. As a consequence, a substantial impact on the regions reconstructed by the experiments T2K and NOvA in the plane of the two parameters  $[\theta_{13}, \delta_{13}]$  is expected. In addition, a similar sensitivity to the two CP-phases  $\delta_{13}$  and  $\delta_{14}$  is expected in the combination of the two LBL experiments with the reactor data.

### 3. Numerical Analysis

In our numerical analysis we include the reactor experiments Daya-Bay and RENO and the two LBL experiments T2K and NOvA. The analysis of LBL data is slightly different for the two cases of three and four flavors, since in this last case there are appreciable oscillation effects not only at the far detector but also at the near detector, which have been taken into account as described in detail in [8].

The analysis of the reactor experiments is performed using the total rate information and following the approach described in [35]. For both experiments we have used the latest data [2, 3] based, respectively, on 621 live days (Daya Bay) and 800 live days (RENO). Since the electron neutrino survival probability probed by these experiments is independent of the CP-violating phases (standard and non-standard), their estimate of  $\theta_{13}$  is independent of them. We recall that such an estimate is extracted using the ratio of the event rates measured at the far and at the near sites. Since the fast oscillations induced by  $\Delta m_{14}^2$  are averaged out at both detector sites, Daya Bay and RENO are not sensitive to 4-flavor effects. As a result, their estimate of  $\theta_{13}$  is independent of the mixing angle  $\theta_{14}$  as long as it is allowed to vary in the range we are exploring.

Concerning the LBL experiments, we use the T2K results of the  $\nu_\mu \rightarrow \nu_e$  appearance searches [1], which reported 28 events with an estimated background of 4.92 events and the preliminary results of the  $\bar{\nu}_\mu \rightarrow \bar{\nu}_e$  searches presented at the EPS HEP conference [10, 11], which report 3 events with an estimated background of 1.68 events. For NOvA we use the preliminary results presented at Fermilab [12]. It must be noticed that the NOvA collaboration, prior to unbinding the data, decided to show the results obtained with two different event selection procedures (LID and LEM). The first is considered the primary method by the collaboration so we conservatively use the results obtained with such a method, which selects 6 events over an estimated background of 0.94 events. For completeness, we will

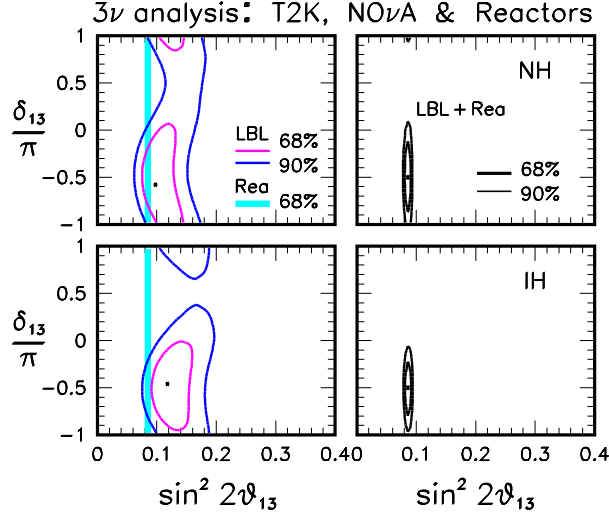


Figure 1: Left panels: regions allowed by the LBL experiments T2K and NOνA and by the  $\theta_{13}$ -sensitive reactor experiments for normal hierarchy (upper panel) and inverted hierarchy (lower panel). Right panels: regions allowed by their combination. The mixing angle  $\theta_{23}$  is marginalized away. The confidence levels refer to 1 d.o.f. ( $\Delta\chi^2 = 1.0, 2.71$ ).

comment on the results that are obtained by using the secondary LEM selector, which identifies a considerably larger number (11) of events (the background being very similar to the LID case) in comparison to the primary LID method.

In order to calculate the theoretical expectation for the total number of T2K  $\nu_e$  events and their binned spectrum in the reconstructed neutrino energy, we convolve the product of the  $\nu_\mu$  flux [36] with horns operating in the +250 kA mode (tables provided on the T2K home page [37]), the charged current quasi elastic (CCQE) cross-section (estimated from [1]), and the  $\nu_\mu \rightarrow \nu_e$  transition probability, with an appropriate energy resolution function. A similar procedure is followed for the antineutrino channel, where we have used the  $\bar{\nu}_\mu$  fluxes with horns operating in the -250 kA mode plotted in [11]. Concerning NOνA we used directly the product of the neutrino fluxes with the cross section (extrapolated at the far detector) provided in [12]. We have checked that our prediction for the binned spectra of events are in good agreement with those shown by the collaborations. We have performed the 3-flavor analysis both using the total rate information and the full spectrum, observing very small differences between the two methods. This is due to the limited statistics currently available, and to the effect of the smearing induced by the energy resolution. As explained in [8], in the 4-flavor case, from outside the collaborations, it is possible to consistently perform only a total rate analysis. Therefore, for homogeneity, also in the 3-flavor case, we report the results obtained with the total rate information.

### 3.1. Results of the 3-flavor analysis

In the 3-flavor analysis, the two mixing angles ( $\theta_{13}$ ,  $\theta_{23}$ ) and the CP-phase  $\delta_{13}$  are treated as free parameters, taking into account the external prior  $\sin^2 \theta_{23} = 0.51 \pm 0.05$  provided by the  $\nu_\mu \rightarrow \nu_\mu$  disappearance measurement [38]

performed by T2K. For the atmospheric mass splitting we use the best fit value  $|\Delta m_{13}^2| = 2.4 \times 10^{-3} \text{ eV}^2$  obtained in the same analysis. The solar mass-mixing parameters are fixed at the best fit value obtained in the global analysis [5].

Figure 1 shows the results of the analysis for the two cases of NH (upper panels) and IH (lower panels) in the plane spanned by the two variables  $[\sin^2 2\theta_{13}, \delta_{13}]$ , the atmospheric mixing angle  $\theta_{23}$  having been marginalized away. The left panels report the regions allowed by the combination of T2K ( $\nu_e$  and  $\bar{\nu}_e$ ) and NOvA ( $\nu_e$ ) for the confidence levels 68% and 90% (1 d.o.f.). When possible [T2K ( $\nu_e$ ) and NOvA ( $\nu_e$ )], we have verified that the results of our analysis obtained for the single experiments in each channel return basically the contour plots presented by the collaborations. The narrow vertical band displayed in both panels represents the range allowed at 68% C.L. for  $\theta_{13}$  by the reactor experiments. It is interesting to note that at the 68% C.L., the contours determined by the combination of T2K and NOvA are closed regions around the best fit value  $\delta_{13} \simeq -\pi/2$ . This means, that thanks to the information coming from the two channels ( $\nu_\mu \rightarrow \nu_e$  and  $\bar{\nu}_\mu \rightarrow \bar{\nu}_e$ ) the LBL experiments are starting to probe the CP symmetry in a *direct* way. This situation is qualitatively different from the preexisting one, where the extraction of the information on  $\delta_{13}$  was *indirect*, i.e. not based upon a manifest observation of CPV. In fact, the previous hints in favor of  $\delta_{13} \simeq -\pi/2$  derived from the combination of T2K ( $\nu_e$ ) and reactor data.

Fig. 1 shows appreciable differences between the two cases of NH and IH, which can be traced to the presence of the matter effects. As discussed in Sec. II, these tend to increase (decrease) the theoretically expected  $\nu_e$  rate in the case of NH (IH). The opposite is true for  $\bar{\nu}_e$ 's but their weight in the analysis is small, so the neutrino datasets dominate. In addition, as discussed in Sec. II, the NOvA  $\nu_e$  data are more sensitive than the T2K  $\nu_e$  data to the matter effects. Therefore, the neutrino datasets are far more relevant for what concern the sensitivity to NMH. More specifically, the following differences among the two hierarchies emerge, which will persist also in the 4-flavor analysis. The regions obtained for the case of IH: i) are shifted towards larger values of  $\theta_{13}$ . ii) are slightly wider in the variable  $\theta_{13}$  with respect to those obtained in the NH case, and iii) tend to prefer (reject) values of  $\sin \delta_{13} < 0$  ( $\sin \delta_{13} > 0$ ) in a more pronounced way.

The two right panels of Fig. 1 show that the combination of the reactor experiments with LBLs tends to further reinforce the preference for values of  $\delta \sim -\pi/2$ , disfavoring the case of no CPV ( $\delta_{13} = 0, \pi$ ) at roughly the 90% C.L. In addition, we note that the weak preference for the case of normal hierarchy tends to consolidate, being  $\chi_{\text{NH}}^2 - \chi_{\text{IH}}^2 \simeq -1.3$ , to be compared with the result  $\chi_{\text{NH}}^2 - \chi_{\text{IH}}^2 = -0.8$  obtained in our previous work [8]. However, the statistical significance of the indication is still small and below the 90% C.L.

A final remark is in order concerning the two events selection methods used by NOvA. As already stressed above, we have conservatively adopted the results obtained with the primary selector, based on a likelihood identification (LID) method. By adopting the results obtained with the alternative method, based on a library event matching (LEM)



selector, which identifies a relatively larger number of  $\nu_e$  events (11 vs 6), we find that both the indication on the CP-phase  $\delta_{13}$  and that on the NMH are slightly enhanced. More precisely, the rejection of the CP-conservation cases ( $\delta_{13} = 0, \pi$ ) and the rejection of the inverted hierarchy both rise, respectively, at about the  $2\sigma$  level and  $1.5\sigma$  level. A combination of the results obtained with the two events selection methods is not trivial because they are strongly correlated. However, one can guess that such a combined analysis would provide results which are intermediate between those obtained using the two methods.

### 3.2. Results of the 4-flavor analysis

Figure 2 displays the results of the 4-flavor analysis for the case of NH. The four panels represent the regions allowed by T2K + NOvA in the usual plane  $[\sin^2 \theta_{13}, \delta_{13}]$  for four different choices of the new CP-phase  $\delta_{14}$ . We have fixed the four-flavor parameters at the following values:  $s_{14}^2 = s_{24}^2 = 0.025$ ,  $s_{34}^2 = 0$ ,  $\delta_{34} = 0$  and  $\Delta m_{14}^2 = 1 \text{ eV}^2$ . As a benchmark we also report the range allowed for  $\theta_{13}$  by reactors, which is identical to the standard case. A quick comparison of the four panels of Fig. 2 with the 3-flavor case (left upper panel of Fig. 1) shows the noticeable impact of the 4-flavor effects on the allowed regions. The behavior of the curves can be qualitatively understood taking into account that the dominant contribution to the total rate comes from a region of the energies close to the first oscillation maximum, where  $\Delta \sim \pi/2$ , and that the neutrino datasets dominate over the antineutrino one. Inspection of Eq. (6) shows that the standard interference term is proportional to  $-\sin \delta_{13}$ . From Eq. (7) we see that for  $\delta_{14} = \pi/2$ , the new interference term is proportional to  $\sin \delta_{13}$ . Therefore, in this case the two terms are in opposition of phase and having similar amplitude tend to cancel out, making the wiggles structure almost to disappear (right upper panel). Vice versa, for  $\delta_{14} = -\pi/2$  (right lower panel) the two interference terms have the same phase and the horizontal excursion of the “wiggles” is increased. In the two cases  $\delta_{14} = 0, \pi$  (left panels) the new interference term is proportional to  $\pm \cos \delta_{13} = \pm \sin(\pi/2 - \delta_{13})$  and thus it has a  $\pm\pi/2$  difference of phase with respect to the standard one. As a result, in such two cases, the behavior of the allowed regions is intermediate between the two cases  $\delta_{14} = (-\pi/2, \pi/2)$ .

Figure 3 shows the allowed regions for the case of IH. For each choice of  $\delta_{14}$ , when going from NH to IH one finds similar changes to those already discussed for the 3-flavor case (shift of  $\theta_{13}$  towards larger values, a wider allowed range for  $\theta_{13}$  and a more pronounced preference for  $\sin \delta_{13} < 0$ ). The changes induced by the hierarchy swap are similar to the 3-flavor case because the matter effects enter in the same way in the 3-flavor case and in the 4-flavor one, i.e. modifying the dominant atmospheric term in the transition probability [see Eq. (13)].

It is interesting to note how, in the presence of  $4\nu$  effects, a better agreement among the two estimates of  $\theta_{13}$  derived from reactors and LBLs can be obtained. In particular, this occurs for  $\delta_{14} \simeq -\pi/2$ . As we have discussed for the 3-flavor case, the mismatch of the  $\theta_{13}$  estimates from LBLs and reactors tends to disfavor the inverted hierarchy. The same is no more true in the 4-flavor scheme, since the two estimates can be brought in agreement for an appro-

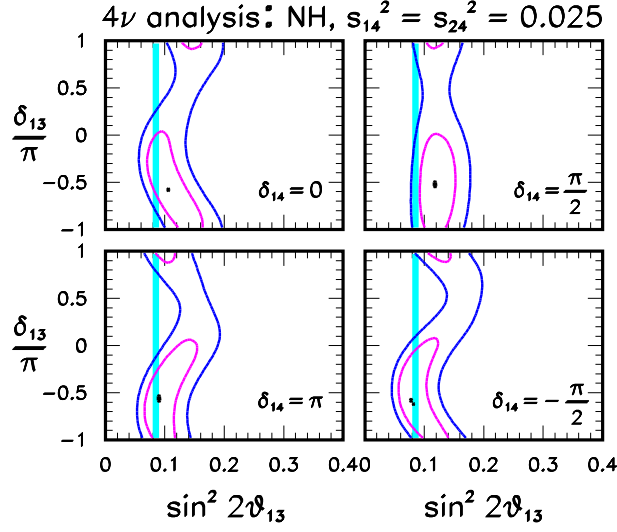


Figure 2: Regions allowed by the combination of T2K and NOvA for four representative values of the CP-phase  $\delta_{14}$ . Normal hierarchy is assumed. The mixing angle  $\theta_{23}$  is marginalized away. The vertical band represents the region allowed by reactor experiments. The confidence levels are as in Fig. 1.

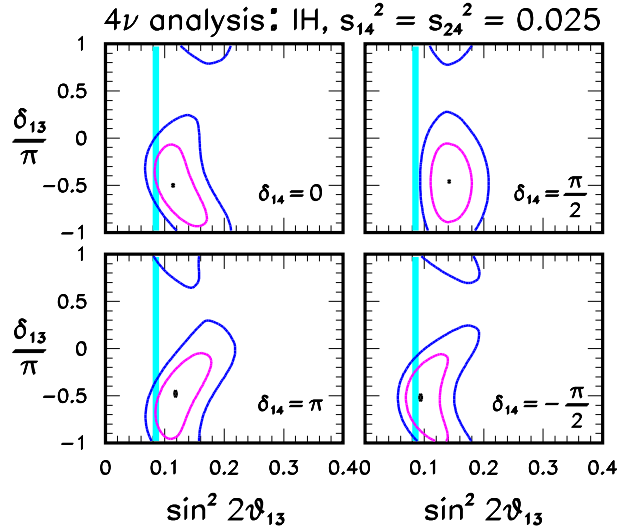


Figure 3: Regions allowed by the combination of T2K and NOvA for four representative values of the CP-phase  $\delta_{14}$ . Inverted hierarchy is assumed. The mixing angle  $\theta_{23}$  is marginalized away. The vertical band represents the region allowed by reactor experiments. The confidence levels are as in Fig. 1.

priate choice of the new CP-phase ( $\delta_{14} \simeq -\pi/2$ ) (see the right bottom panel of 3). This circumstance indicates that light sterile neutrinos may constitute a potential source of fragility in the capability of the two LBL experiments of discriminating the neutrino mass hierarchy.

As a last step in our 4-flavor analysis, we perform the combination of LBLs with reactors. In this more general analysis, we treat the two mixing angles ( $\theta_{13}, \theta_{23}$ ) and the two CP-phases ( $\delta_{13}, \delta_{14}$ ) as free parameters, while fixing the remaining 4-flavor parameters at the same values used before:  $s_{14}^2 = s_{24}^2 = 0.025$ ,  $s_{34}^2 = 0$ ,  $\delta_{34} = 0$  and  $\Delta m_{14}^2 = 1 \text{ eV}^2$ .

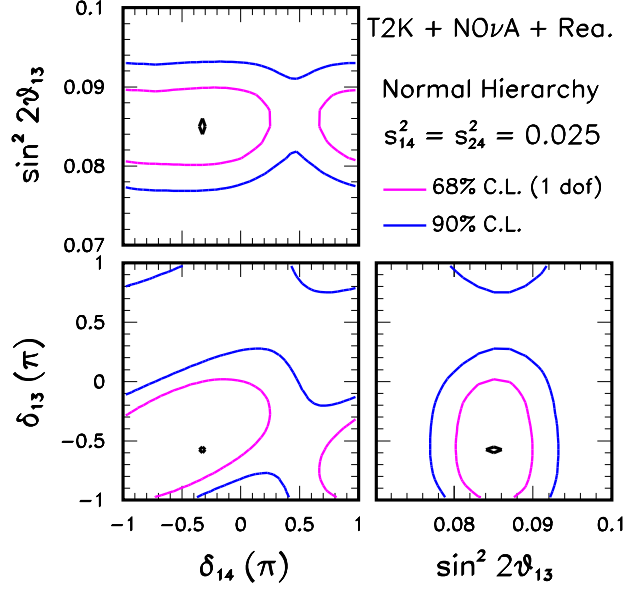


Figure 4: Regions allowed by the combination of the LBL experiments and the reactor experiments for the case of normal hierarchy. The mixing angle  $\theta_{23}$  is marginalized away.

We have checked that the impact of non-zero  $\theta_{34}$  (and consequently of the associated CP-phase  $\delta_{34}$ ) is negligible when considering values of  $\theta_{34}$  below the current upper bounds.

Similarly to the 3-flavor case, in the LBL + Reactor combination, the (CP-phases independent) estimate of  $\theta_{13}$  provided by the reactor experiments selects those subregions of the LBL bands which have a statistically significant overlap with such an estimate. These, in turn, correspond to allowed regions in the plane  $[\delta_{13}, \delta_{14}]$  spanned by the two CP-phases. Figures 4 and 5 display such regions for the two cases of NH and IH, together with the 2-dimensional projections having as one of the two variables the mixing angle  $\theta_{13}$ . As expected, there is a similar sensitivity to both CP-phases with a preference for values of  $\delta_{13} \sim \delta_{14} \sim -\pi/2$ . The case  $\delta_{13} = 0$  is disfavored at a slightly lower confidence level in comparison with the 3-flavor case. This is imputable to the degeneracy among the two CP-phases.

#### 4. Conclusions and Outlook

We have investigated the impact of the latest data released by the two long-baseline experiments T2K and NOνA. Specifically, we have included in our analysis the first  $\bar{\nu}_e$  appearance data from T2K and the first  $\nu_e$  appearance results from NOνA. We have considered the implications of such new results both for the standard 3-flavor framework and for the non-standard 3+1 scheme involving one sterile neutrino species, which is the most popular scenario invoked to explain the short-baseline anomalies (see [39, 40, 41]).

The 3-flavor analysis shows a consolidation of the preexisting trends, namely a slight preference for  $\sin \delta_{13} < 0$

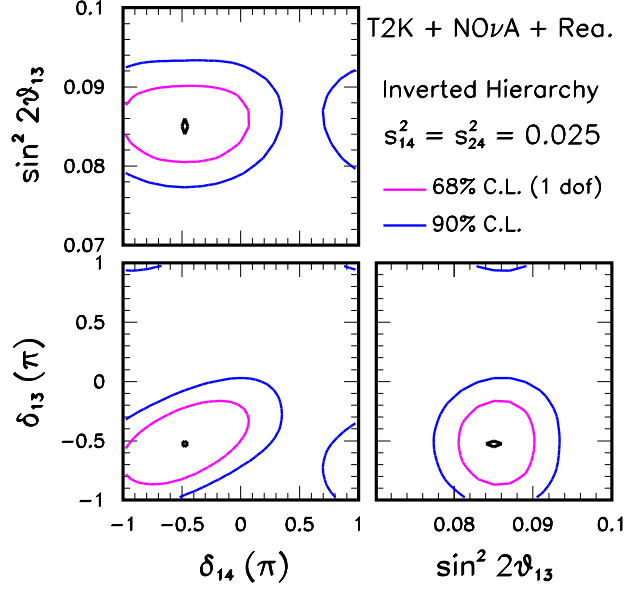


Figure 5: Regions allowed by the combination of the LBL experiments and the reactor experiments for the case of inverted hierarchy. The mixing angle  $\theta_{23}$  is marginalized away.

disfavoring the cases of CP conservation ( $\delta = 0, \pi$ ) at a confidence level close to 90% C.L., and a mild preference (at more than 68% C.L.) for the normal hierarchy. These hints are slightly reinforced if one adopts the NO $\nu$ A results obtained with the secondary event selection method (LEM). In a 3+1 framework, two CP-phases ( $\delta_{13} \equiv \delta$  and  $\delta_{14}$ ) are constrained, which exhibit a preference for the common value  $\delta_{13} \simeq \delta_{14} \simeq -\pi/2$ . Interestingly, in the enlarged four neutrino scheme the preference for the NH found within the 3-flavor framework completely disappears because the mismatch between the two estimates of  $\theta_{13}$  from LBL's and reactors can be lifted (an intriguing circumstance) if the new CP-phase  $\delta_{14}$  lies around its best value  $-\pi/2$ . This fact indicates that light sterile neutrinos may constitute a potential source of fragility in the capability of the two LBL experiments of discriminating between the two neutrino mass hierarchies.

Our results show once again that LBL experiments can give an important contribution in the context of sterile neutrino searches, which should not be considered only a short-baseline “affair”. In particular, no information on the new CP-phase  $\delta_{14}$  can be extracted from SBL setups, where the interference between the new splitting and the atmospheric one cannot develop (or is completely negligible). Therefore, the two classes of experiments (SBL and LBL) are complementary and synergic in constraining the 4-flavor parameter space. While a discovery of a sterile neutrino can come only from the observation of the oscillating pattern (in energy or/and space) at the new SBL experiments, the full exploration of the 4 $\nu$  model will become possible only with the contribution of LBL setups, which are sensible interferometers able to probe the new enlarged CPV sector. Also the (present and future) atmospheric neutrino data

may help to shed light on this issue, since these neutrinos traverse very long baselines and may present some sensitivity to the new CPV phenomena.

Finally, we would like to underline the other side of the coin, namely the fact that the presence of sterile neutrinos tend to decrease the robustness of the conclusions reached in the simple 3-flavor framework. The present data already show that this is the case for the current hint in favor of NH, which disappears in the 3+1 scheme. In this respect, it would be very interesting to study how the NMH discrimination capabilities of future data expected to come from T2K and NO $\nu$ A, and from the planned LBL experiments (DUNE, LBNO and T2HK) will be affected by the inclusion of the sterile neutrino effects.

## Acknowledgments

We thank M. Ravonel Salzgeber for information on the T2K electron antineutrino data. We are grateful to the organizers of the 14<sup>th</sup> *Conference on Topics in Astroparticle and Underground Physics* held in Turin – where preliminary results of this work were presented – for kind hospitality. We acknowledge support from the Grant “Future In Research” *Beyond three neutrino families*, contract no. YVI3ST4, of Regione Puglia, Italy. We acknowledge partial support from the EU though the FP7 ITN “Invisibles” (PITN-GA-2011-289442).

## References

- [1] K. Abe *et al.* [T2K Collaboration], Phys. Rev. Lett. **112**, 061802 (2014) [arXiv:1311.4750 [hep-ex]].
- [2] L. Zhan [Daya Bay Collaboration], arXiv:1506.01149 [hep-ex].
- [3] Soo-Bong Kim [RENO Collaboration], talk given at the International Conference on Neutrinos and Dark Matter in Nuclear Physics, Jyväskylä, Finland, June 1-5, 2015.
- [4] Y. Abe *et al.* [Double Chooz Collaboration], JHEP **1410**, 86 (2014) [arXiv:1406.7763 [hep-ex]].
- [5] F. Capozzi, G. L. Fogli, E. Lisi, A. Marrone, D. Montanino and A. Palazzo, Phys. Rev. D **89** (2014) 093018 [arXiv:1312.2878 [hep-ph]].
- [6] J. Bergstrom, M. C. Gonzalez-Garcia, M. Maltoni and T. Schwetz, arXiv:1507.04366 [hep-ph].
- [7] D. V. Forero, M. Tortola and J. W. F. Valle, Phys. Rev. D **90**, 093006 (2014) [arXiv:1405.7540 [hep-ph]].
- [8] N. Klop and A. Palazzo, Phys. Rev. D **91**, no. 7, 073017 (2015) [arXiv:1412.7524 [hep-ph]].
- [9] J. Elevant and T. Schwetz, arXiv:1506.07685 [hep-ph].
- [10] M. R. Salzgeber [T2K Collaboration], talk given at European Physical Society HEP conference, Vienna, 22-29 July 2015.
- [11] M. R. Salzgeber [T2K Collaboration], arXiv:1508.06153 [hep-ex].
- [12] R. Patterson [NO $\nu$ A Collaboration], talk given at the Joint Experimental-Theoretical Physics Seminar, Fermilab, 6 August 2015.
- [13] D. Hollander and I. Mocioiu, arXiv:1408.1749 [hep-ph].
- [14] J. M. Berryman, A. de Gouvea, K. J. Kelly and A. Kobach, arXiv:1507.03986 [hep-ph].
- [15] R. Gandhi, B. Kayser, M. Masud and S. Prakash, arXiv:1508.06275 [hep-ph].
- [16] A. Donini and D. Meloni, Eur. Phys. J. C **22**, 179 (2001) [hep-ph/0105089].

- [17] A. Donini, M. Lusignoli and D. Meloni, Nucl. Phys. B **624**, 405 (2002) [hep-ph/0107231].
- [18] A. Donini, M. Maltoni, D. Meloni, P. Migliozzi and F. Terranova, JHEP **0712** (2007) 013 [arXiv:0704.0388 [hep-ph]].
- [19] A. Dighe and S. Ray, Phys. Rev. D **76**, 113001 (2007) [arXiv:0709.0383 [hep-ph]].
- [20] A. Donini, K. i. Fuki, J. Lopez-Pavon, D. Meloni and O. Yasuda, JHEP **0908**, 041 (2009) [arXiv:0812.3703 [hep-ph]].
- [21] O. Yasuda, arXiv:1004.2388 [hep-ph].
- [22] D. Meloni, J. Tang and W. Winter, Phys. Rev. D **82**, 093008 (2010) [arXiv:1007.2419 [hep-ph]].
- [23] B. Bhattacharya, A. M. Thalapillil and C. E. M. Wagner, Phys. Rev. D **85**, 073004 (2012) [arXiv:1111.4225 [hep-ph]].
- [24] A. Donini, P. Hernandez, J. Lopez-Pavon, M. Maltoni and T. Schwetz, JHEP **1207**, 161 (2012) [arXiv:1205.5230 [hep-ph]].
- [25] L. Wolfenstein, Phys. Rev. D **17**, 2369 (1978).
- [26] S. P. Mikheev and A. Yu. Smirnov, Yad. Fiz. **42**, 1441 (1985) [Sov. J. Nucl. Phys. **42**, 913 (1985)].
- [27] M. G. Aartsen *et al.* [IceCube PINGU Collaboration], arXiv:1401.2046 [physics.ins-det].
- [28] U. F. Katz [KM3NeT Collaboration], [arXiv:1402.1022 [astro-ph.IM]].
- [29] K. Abe *et al.*, arXiv:1109.3262 [hep-ex].
- [30] S. Ahmed *et al.* [ICAL Collaboration], arXiv:1505.07380 [physics.ins-det].
- [31] G. L. Fogli, E. Lisi, A. Marrone and A. Palazzo, Prog. Part. Nucl. Phys. **57**, 742 (2006) [hep-ph/0506083].
- [32] A. Cervera, A. Donini, M. B. Gavela, J. J. Gomez Cadenas, P. Hernandez, O. Mena and S. Rigolin, Nucl. Phys. B **579**, 17 (2000) [Erratum-  
ibid. B **593**, 731 (2001)] [hep-ph/0002108].
- [33] K. Asano and H. Minakata, JHEP **1106**, 022 (2011) [arXiv:1103.4387 [hep-ph]].
- [34] T. Kikuchi, H. Minakata and S. Uchinami, JHEP **0903**, 114 (2009) [arXiv:0809.3312 [hep-ph]].
- [35] A. Palazzo, JHEP **1310**, 172 (2013) [arXiv:1308.5880 [hep-ph]].
- [36] K. Abe *et al.* [T2K Collaboration], Phys. Rev. D **87**, 012001 (2013) [arXiv:1211.0469 [hep-ex]].
- [37] <http://t2k-experiment.org/results/neutrino-beam-flux-2013/>
- [38] K. Abe *et al.* [T2K Collaboration], Phys. Rev. Lett. **112**, no. 18, 181801 (2014) [arXiv:1403.1532 [hep-ex]].
- [39] A. Palazzo, Mod. Phys. Lett. A **28**, 1330004 (2013) [arXiv:1302.1102 [hep-ph]].
- [40] J. Kopp, P. A. N. Machado, M. Maltoni and T. Schwetz, JHEP **1305**, 050 (2013) [arXiv:1303.3011 [hep-ph]].
- [41] C. Giunti, M. Laveder, Y. F. Li and H. W. Long, Phys. Rev. D **88**, 073008 (2013) [arXiv:1308.5288 [hep-ph]].